Distinct recognition of complement iC3b by integrins $\alpha_X\beta_2$ and $\alpha_M\beta_2$

Shutong Xu[a,1], Jianchuan Wang[b,1], Jia-Huai Wang[a,c,2], and Timothy A. Springer[b,2]

[a]Department of Medical Oncology, Dana-Farber Cancer Institute, Boston, MA 02215; [b]Program in Cellular and Molecular Medicine, Boston Children's Hospital and Department of Biological Chemistry and Molecular Pharmacology, Harvard Medical School, Boston, MA 02115; and [c]Department of Pediatrics, and Biological Chemistry and Molecular Pharmacology, Harvard Medical School, Boston, MA 02215

Contributed by Timothy A. Springer, February 2, 2017 (sent for review December 2, 2016; reviewed by Anne Nicholson-Weller and Thomas Vorup-Jensen)

Recognition by the leukocyte integrins $\alpha_X\beta_2$ and $\alpha_M\beta_2$ of complement iC3b-opsonized targets is essential for effector functions including phagocytosis. The integrin-binding sites on iC3b remain incompletely characterized. Here, we describe negative-stain electron microscopy and biochemical studies of $\alpha_X\beta_2$ and $\alpha_M\beta_2$ in complex with iC3b. Despite high homology, the two integrins bind iC3b at multiple distinct sites. $\alpha_X\beta_2$ uses the α_X αI domain to bind iC3b on its C3c moiety at one of two sites: a major site at the interface between macroglobulin (MG) 3 and MG4 domains, and a less frequently used site near the C345C domain. In contrast, $\alpha_M\beta_2$ uses its αI domain to bind iC3b at the thioester domain and simultaneously interacts through a region near the α_M β-propeller and β_2 βI domain with a region of the C3c moiety near the C345C domain. Remarkably, there is no overlap between the primary binding site of $\alpha_X\beta_2$ and the binding site of $\alpha_M\beta_2$ on iC3b. Distinctive binding sites on iC3b by integrins $\alpha_X\beta_2$ and $\alpha_M\beta_2$ may be biologically beneficial for leukocytes to more efficiently capture opsonized pathogens and to avoid subversion by pathogen factors.

Activation of mammalian complement is critical for the clearance of pathogens and altered host cells, whereas excessive activation results in tissue damage (1). Complement activation can be initiated by three distinct pathways with proteolytic cleavage of complement component C3 as the pivotal step in each pathway. C3 is cleaved to C3b by C3 convertases. C3b participates in some C3 convertases to amplify C3 cleavage; however, further cleavage of C3b to iC3b inactivates convertase activity. In turn, iC3b can be digested to yield C3c plus C3dg, and C3dg can be further cleaved to C3d (2) (Fig. 1*A*). Conversion of C3 to C3b exposes the otherwise buried reactive thioester bond in the thioester domain (TED) and enables it to covalently attach to hydroxyl and amino groups on pathogenic, immunogenic, and apoptotic cell surfaces (3). Opsonic fragments of C3 covalently bound through the TED, i.e., C3b, iC3b, and C3dg/C3d serve as ligands for five distinct complement receptors (CRs). Each CR has been characterized for its preference for specific C3 opsonic fragments. CR type 3 (CR3, also known as CD11b/CD18, Mac-1, or integrin $\alpha_M\beta_2$) and CR type 4 (CR4, also known as CD11c/CD18, p150, 95, or integrin $\alpha_X\beta_2$) specifically recognize iC3b as shown by selective rosette formation with erythrocytes opsonized with iC3b but not C3b or C3d (4–6), and specific isolation from cells by affinity chromatography on iC3b-Sepharose beads (7). However, at high concentrations on opsonized cells, C3d and C3dg can show reactivity with CR3 (8, 9).

$\alpha_X\beta_2$ and $\alpha_M\beta_2$ are heterodimeric proteins belonging to the β_2 integrin subfamily. They are expressed on myeloid cells including neutrophil granulocytes, monocytes, macrophages, and also on activated lymphocytes and lymphoid natural killer cells (10–12). $\alpha_X\beta_2$ and $\alpha_M\beta_2$ are essential for recognition and phagocytosis of pathogens and immune complexes in vivo (13). Deficiency of $\alpha_X\beta_2$ and $\alpha_M\beta_2$ in leukocyte adhesion deficiency results in recurring bacterial infections (14) and deficiency of $\alpha_M\beta_2$ alters susceptibility to injury from immune complexes (15). The β_2-associated α subunits all contain an inserted domain (αI domain), which adopts a Rossmann fold with a metal ion-dependent adhesion site (MIDAS) at the ligand-binding site (Fig. 1*B*) (16).

The αI domain of $\alpha_X\beta_2$ and $\alpha_M\beta_2$ plays a key role in recognition of iC3b by both integrins; however, alternative recognition modes have also been suggested. Mutagenesis and antibody blocking studies on $\alpha_X\beta_2$ and $\alpha_M\beta_2$ showed that the αI domain was required for binding to iC3b (6, 17, 18). More recently, electron microscopy (EM) studies with the $\alpha_X\beta_2$ ectodomain revealed binding solely through its αI domain to a site at the interface between the macroglobulin (MG) 3 and MG4 domains on the C3c moiety of iC3b (Fig. 1*A*) (19). However, stoichiometry suggests multiple binding sites for the α_X αI domain in iC3b (20). Because of the high similarity between $\alpha_X\beta_2$ and $\alpha_M\beta_2$, it was expected that $\alpha_M\beta_2$ would bind to the same site on iC3b as $\alpha_X\beta_2$. It was surprising then when a crystal structure of a complex between the α_M αI domain and TED (C3d) revealed a specific complex between them (21). As the authors pointed out, binding of the α_M αI domain alone to TED could not explain the specificity of $\alpha_M\beta_2$ for binding to iC3b and not to C3d (21). Moreover, the α_M subunit β-propeller domain and the β_2 subunit inserted domain (βI) (Fig. 1*B*) have been suggested to additionally contribute to iC3b binding (22–24). Both $\alpha_M\beta_2$ and $\alpha_X\beta_2$ recognize a variety of unrelated ligands and proteolyzed or denatured proteins (25); given this broad specificity, $\alpha_X\beta_2$ has been termed a "danger receptor" (26). Furthermore, the isolated α_M αI domain has been crystallized in the open conformation bound to a neighboring αI domain in a ligand-mimetic lattice contact (27). Thus, it was interesting to determine whether the α_M αI domain complex with the TED domain in crystals (21) could be extended to larger integrin and complement fragments and whether additional contacts might be found. These findings

Significance

Complement is deposited on foreign antigens and particles and marks them for recognition by immune cells and removal by phagocytes. Immune cells have two homologous integrins, $\alpha_X\beta_2$ and $\alpha_M\beta_2$, that recognize the complement fragment iC3b. Although it might have been suspected that these integrins would bind to the same site on iC3b, direct comparisons here show they do not. Using negative stain electron microscopy and purified integrin fragments and iC3b, we show that $\alpha_X\beta_2$ binds to two distinct sites on iC3b. A single $\alpha_M\beta_2$ integrin binds to two different sites on iC3b, each of which is distinct from those to which $\alpha_X\beta_2$ binds. Our findings reveal remarkable diversity among integrins that recognize complement and suggest possible cooperative responses.

Author contributions: S.X., J.W., J.-H.W., and T.A.S. designed research; S.X. and J.W. performed research; S.X., J.W., J.-H.W., and T.A.S. analyzed data; and S.X., J.W., J.-H.W., and T.A.S. wrote the paper.

Reviewers: A.N.-W., Harvard Medical School, Beth Israel Deaconess Medical Center; and T.V.-J., University of Aarhus.

The authors declare no conflict of interest.

[1]S.X. and J.W. contributed equally to this work.

[2]To whom correspondence may be addressed. Email: springer_lab@crystal.harvard.edu or jwang@crystal.harvard.edu.

This article contains supporting information online at www.pnas.org/lookup/suppl/doi:10.1073/pnas.1620881114/-/DCSupplemental.

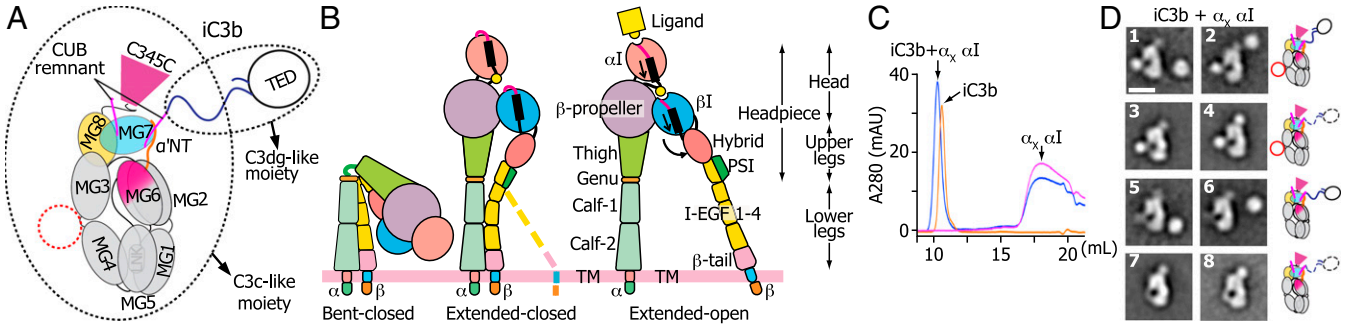

Fig. 1. Integrins, iC3b, and negative-stain EM of α_X I domain and iC3b complexes. (*A*) Schematic of iC3b. (*B*) Schematic of domain organization and conformational states of αI-integrins $\alpha_X\beta_2$ and $\alpha_M\beta_2$. (*C*) Superdex 200 size exclusion chromatography profiles of iC3b in presence or absence of the α_X αI F273S/F300A mutant in presence of 2 mM Mg^{2+}. (*D*) Better resolved class averages of α_X αI and iC3b complexes. (Scale bar: 10 nm.) Schematic interpretations of classes are shown to the right.

also suggested the importance of further comparisons between $\alpha_M\beta_2$ and $\alpha_X\beta_2$, particularly with integrin fragments complementary to those previously used in structural studies, i.e., the ectodomain in the case of $\alpha_X\beta_2$ (19) and the αI domain in the case of $\alpha_M\beta_2$ (21).

Using negative-stain EM with the α_X αI domain and the $\alpha_M\beta_2$ headpiece here, we have shown that $\alpha_X\beta_2$ and $\alpha_M\beta_2$ bind to different regions of iC3b. Distinct recognition modes toward iC3b by two closely related β_2 integrins reveal surprising diversity that might be important for complement recognition in the context of the quite different surfaces or antigens on which complement can be deposited and enable cooperative rather than competitive functions for $\alpha_X\beta_2$ and $\alpha_M\beta_2$.

Results

Interaction of $\alpha_X\beta_2$ with iC3b. To stabilize the high-affinity state of the isolated α_X αI domain (α_X residues E130-G319), we introduced mutations F273S and F300A. Homologous mutations F265S and F292A had been found by random mutagenesis followed by directed evolution to increase the affinity of the α_L αI domain and stabilize its open conformation (28). The corresponding residues in α_X have identical structural environments, which suggested that their mutation should similarly stabilize the open, high-affinity conformation. Indeed, the F273S/F300A α_X αI domain, used in all studies below, formed a complex with iC3b that was stable to gel filtration in buffer containing 2 mM Mg^{2+} and eluted earlier than iC3b alone (Fig. 1*C*). In contrast, the wild-type $\alpha_X\beta_2$ ectodomain required not only the activating metal ion Mn^{2+}, but also Fabs that stabilize the open integrin headpiece conformation (Fig. 1*B*), to form complexes with iC3b that were stable to gel filtration (19).

The isolated α_X αI complex with iC3b was subjected to negative-stain EM with multivariate K-means classification and multi-reference alignment of >5,000 particles into 50 class averages (Fig. S1). Class averages were visualized corresponding to both the α_X αI domain bound to iC3b (Fig. 1*D*, *1–4*) and iC3b alone (Fig. 1*D*, *5–8*). The α_X αI domain bound to the key ring moiety formed by MG domains 1–8 of iC3b (Fig. 1 *A* and *D*). The key ring moiety can be oriented both (*i*) by its weaker density on the side with only MG3 and MG4 compared with the thicker density on the side where MG1 and MG2 stack atop MG5 and MG6 and (*ii*) by the slant of the C345C knob toward the thick side (Fig. 1*A*). This orientation confirmed binding of the αI domain to MG3 and MG4 near their interface (Fig. 1*D*, *1–4* and schematics).

In conversion from C3b to iC3b, factor I cleaves the CUB domain in its C-terminal linkage to TED. Cleavage leaves TED tethered to the C3c moiety through its N-terminal linkage. In agreement with previous results (29), we found that the TED is flexibly tethered to the C3c moiety in iC3b, as shown by its appearance in different orientations and distances relative to the C3c moiety (Fig. 1*D*, *1, 2, 5,* and *6*) and its lack of defined orientation (absence of density) in other class averages (Fig. 1*D*, *3, 4, 7,* and *8*). The TED (296 residues) was clearly distinguished by its stronger density from the smaller αI domain (190 residues) (Fig. 1*D*).

Interaction of $\alpha_X\beta_2$ with C3c. Further cleavage by factor I of iC3b in the CUB domain separates TED (C3dg) from C3c. We prepared α_X αI domain complexes with C3c in Mg^{2+} by gel filtration (Fig. 2*A*) and characterized them by EM (Fig. 2*B* and Fig. S2*A*) using the same methods as described above for iC3b. Although some particles showed C3c alone (Fig. 2*B*, *1* and *2*), most (30 classes, corresponding to 68% of particles) showed αI bound near the MG3-MG4 interface on the MG key ring (Fig. 2*B*, *3–8*). Strikingly, at least 8 of 50 class averages showed an additional density for αI near the C345C knob (Fig. 2*B*, *5–8*).

In five class averages (9.5% of particles), the second αI domain appeared on the thick side of the MG key ring (Fig. 2*B*, *5* and *6*), whereas in others (3.3% of particles), it appeared on the opposite side of the C345C knob nearer the thin side of the MG key ring (Fig. 2*B*, *7* and *8*). The differing orientations might reflect binding to the flexible remnants of the cleaved CUB domain, which localize near the C345C knob, and/or may reflect a 3D orientation of αI out of the C3c plane visualized in Fig. 2*B* and the tendency of particles to lie flat on EM substrates.

Having found two binding sites for the isolated α_X αI domain in the C3c moiety, we then asked whether two binding sites could also be found with the intact $\alpha_X\beta_2$ ectodomain. We reexamined grids from a published study (19) on C3c complexes formed with the $\alpha_X\beta_2$ ectodomain stabilized in the high-affinity state with three Fab fragments. We found in the same fields from which 4,387 1:1 $\alpha_X\beta_2$:C3c particles had been picked 121 putative 2:1 particles that were classified into two classes (Fig. 2*C* and Fig. S2*B*). Indeed, both class averages revealed 2:1 $\alpha_X\beta_2$ ectodomain-Fab:C3c complexes. The orientations were similar in the two classes (Fig. 2*C*, diagrammed in Fig. 2*F*), although density was clearest in the most populous average (Fig. 2*C*, *1*). Our domain assignments were confirmed by masking all segments except C3c, and cross-correlation with the C3c crystal structure (Fig. 2*C*, *Middle* and *Bottom*). The cross-correlation scores were excellent and were comparable to those using the C3c moiety from 1:1 complexes (Fig. 2*E*, *Middle* and *Bottom*). The orientation of the two integrins in the class averages is readily assigned based on densities for the head containing the αI, β-propeller, and βI domains, and weaker densities for the α- and β-subunit legs. The two integrins orient with their β-subunits facing toward one another as shown by the stronger density of the large β-propeller domain, which marks the α-subunit side of the head, and m24 Fab, which binds to the βI domain and marks the β-subunit side of the head (Fig. 2 *C* and *F*). Importantly, these landmarks, and the densities for the two αI domains, confirm that the αI domain in one integrin binds near the

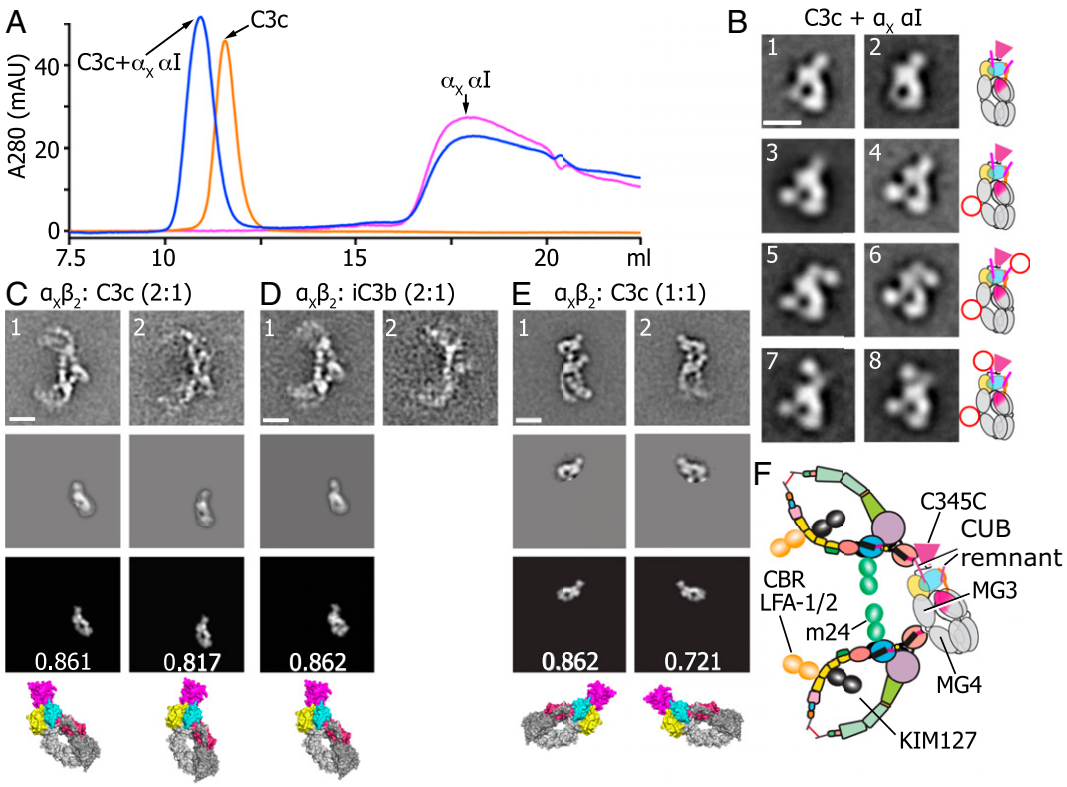

Fig. 2. Negative-stain EM of α_X αI domain complexes with C3c and comparison with $\alpha_X\beta_2$ ectodomain complexes with C3c and iC3b. (*A*) Superdex 200 size exclusion chromatography profiles of C3c, the α_X αI F273S/F300A mutant, or their mixture in presence of 2 mM Mg^{2+}. (*B*) Better resolved class averages of α_X αI and C3c complexes. Schematic interpretations of the averages are shown to the right. (*C*–*E*) Complexes (2:1) containing two integrin $\alpha_X\beta_2$ ectodomains bound to C3c (*C*) or iC3b (*D*) or for comparison 1:1 $\alpha_X\beta_2$:C3c class averages (*E*) (19). The 2:1 complexes were identified among published 1:1 complexes (19) as described in *Results*. To confirm the position of the C3c or the C3c moiety of iC3b in the class averages (*Top*), class averages were masked (*Middle*) and cross-correlated with a C3c crystal structure (*Bottom*) with cross-correlation score and C3c ribbon cartoon shown below. (Scale bars: 10 nm.) (*F*) Schematic of 2:1 complexes. Three Fabs bound to $\alpha_X\beta_2$ to stabilize its extended-open conformation are shown. *E* reproduced from ref. 19.

MG3-MG4 interface in the MG key ring and that the αI domain in the other integrin binds near the C345C knob, exactly as described above for isolated α_X αI domains.

We then asked whether 2:1 complexes might be present within $\alpha_X\beta_2$ complexes with iC3b (19). In the same fields from which 5,134 1:1 complexes had been subjected to class averaging (19), we found 161 putative 2:1 complexes that were subjected to classification and averaging into two classes (Fig. 2*D*). The most populous class average showed the same two αI domain sites on iC3b as seen with C3c, with one binding site near the MG3-MG4 interface and the other near the C345C knob (Fig. 2*D*, *1*). The second class average was less clear, although density for m24 Fab bound to each integrin suggested a similar integrin orientation as in the other class average.

Recognition of iC3b but Not C3c by $\alpha_M\beta_2$. A headpiece fragment of $\alpha_M\beta_2$ in 1 mM Mn^{2+} and 0.2 mM Ca^{2+} formed complexes with iC3b that were stable to gel filtration as shown by elution of the complex earlier than iC3b alone or the $\alpha_M\beta_2$ headpiece monomer (Fig. 3 *A* and *C*). EM class averages showed that the $\alpha_M\beta_2$ headpiece bound through its αI domain to the iC3b TED (Fig. 3*D* and Fig. S3*A*). The position of the TED with respect to the C3c moiety of iC3b varied much less in complexes with $\alpha_M\beta_2$ than in complexes with the α_X αI domain or in iC3b alone (Fig. 1*D*) (19, 29). Furthermore, the C3c moiety adopted similar, nonrandom orientations with respect to the integrin, with its C345C knob close to the β-propeller and βI domains in the integrin head (Fig. 3*D*). In some class averages, the knob approached the head closely (Fig. 3*D*, *5* and *6*). The nonrandom orientation of the C3c moiety and close approach of its knob to the integrin strongly suggest a second three-dimensional contact between the integrin and iC3b that is less stable than the αI-TED contact and is susceptible to disruption when complexes adsorb to the grid and become largely planar.

In contrast to iC3b, C3c failed to complex with the $\alpha_M\beta_2$ headpiece (Fig. 3*B*). An early eluting peak was present in samples containing C3c and $\alpha_M\beta_2$ or $\alpha_M\beta_2$ alone, but not in C3c alone (Fig. 3*B*). This peak contained no $\alpha_M\beta_2$–C3c complex but did contain an $\alpha_M\beta_2$ headpiece dimer (Fig. S3*B*) as described in *Dimerization of the $\alpha_M\beta_2$ Headpiece*.

Ligand binding by other αI domain-containing integrins has been associated with headpiece opening, as visualized in EM by swing-out of the hybrid domain (Fig. 1*B*). To determine whether the headpiece was open or closed in $\alpha_M\beta_2$ bound to iC3b, we cross-correlated it to crystal structures or models of the closed and open $\alpha_X\beta_2$ headpiece. Better correlation to the open headpiece revealed that the $\alpha_M\beta_2$ headpiece is open when bound to iC3b (Fig. 3*D*, *Bottom*). Moreover, cross-correlation showed that the headpiece oriented with its β-subunit adjacent to the C3c moiety in all class averages. This nonrandom orientation of the $\alpha_M\beta_2$ headpiece provided further evidence for a specific interaction of its β-propeller and βI domain region with a C345C knob-proximal region of the C3c moiety of iC3b.

Dimerization of the $\alpha_M\beta_2$ Headpiece. When incubated alone in buffer with 1 mM Mn^{2+} and 0.2 mM Ca^{2+}, the $\alpha_M\beta_2$ headpiece readily formed a dimer, as shown both by gel filtration (Fig. 3 *A*–*C*) and EM (Fig. 3*E* and Fig. S3 *B* and *C*). Dimer formation was not seen in buffer with 1 mM Mg^{2+} and 1 mM Ca^{2+} (Fig. 3*C*). When the $\alpha_M\beta_2$ headpiece and iC3b were mixed in buffer with 1 mM Mn^{2+} and 0.2 mM Ca^{2+}, $\alpha_M\beta_2$ complex formation with iC3b was favored over

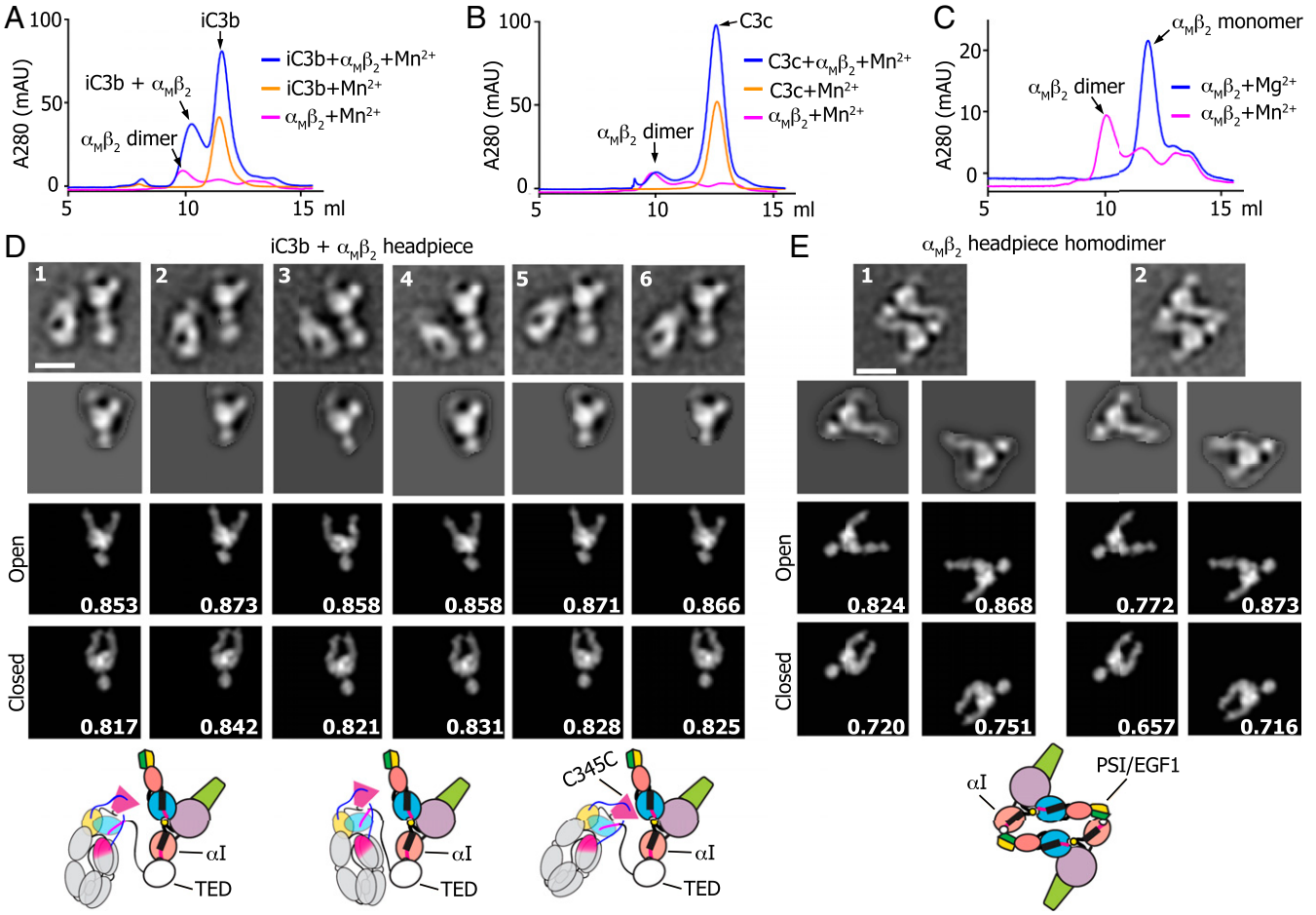

Fig. 3. Negative-stain EM of $\alpha_M\beta_2$ headpiece complexes. (*A–C*) Superdex 200 size exclusion chromatography profiles of complexes and individual components in Mn^{2+} with iC3b (*A*), C3c (*B*), or the $\alpha_M\beta_2$ headpiece alone in Mg^{2+} or Mn^{2+} (*C*). (*D* and *E*) Better resolved class averages of the $\alpha_M\beta_2$ headpiece complex with iC3b (*D*) and $\alpha_M\beta_2$ headpiece homodimer complexes in Mn^{2+} (*E*). To figure out whether the $\alpha_M\beta_2$ headpiece is in open or closed conformation, class averages were masked (row 2) and cross-correlated with a modeled open form $\alpha_x\beta_2$ headpiece (row 3) or a crystal structure of $\alpha_x\beta_2$ headpiece in closed conformation (PDB ID code 4NEH) (row 4). The cross-correlation scores are labeled. The schematic interpretations of the class averages are shown below. (Scale bar: 10 nm.)

$\alpha_M\beta_2$ dimer formation, with only 1 of 50 class averages showing the dimer (Fig. S3*A*). Dimer formation appears to reflect the ability of $\alpha_M\beta_2$ to promiscuously recognize a wide range of ligands (Introduction). $\alpha_M\beta_2$ headpiece dimers displayed dyad symmetry, with the αI domain of one monomer bound to the distal end of the β-leg, i.e., to the I-EGF1 or PSI domain, of the other monomer (Fig. 3*E*, see diagram below). Furthermore, cross-correlation showed that the headpiece was open when one $\alpha_M\beta_2$ monomer bound to another monomer (Fig. 3*E*).

Discussion

Recognition of the complement degradation product iC3b by leukocyte integrins $\alpha_X\beta_2$ and $\alpha_M\beta_2$ is critical for phagocytosis of opsonized foreign particles in host defense. The α_X and α_M subunits are 60% identical in sequence overall, and their αI domains have 57% sequence identity. Based on sequence homology and recognition of the same ligand, it might be expected that $\alpha_X\beta_2$ and $\alpha_M\beta_2$ would bind similarly to iC3b (19). Here, using negative-stain EM, we clearly show that $\alpha_X\beta_2$ and $\alpha_M\beta_2$ bind to distinct sites on iC3b.

Structures of the $\alpha_X\beta_2$ and $\alpha_M\beta_2$ αI domains, including the α_X αI domain trapped in the open conformation by a lattice contact in bent $\alpha_X\beta_2$ ectodomain crystals (30), and of the open α_M αI domain bound to the C3 TED (21) show marked differences that rationalize their differences in specificity. Residues in the α_M αI domain that contact the TED, which lie in loops that surround the MIDAS Mg^{2+} ion, differ completely in α_X. Thus, the most important TED-contacting residues in α_M, with the equivalent α_X residues in parenthesis, are Glu-178 (Asn), Glu-179 (Lys), Leu-206 (Gln), Arg-208 (Phe), and Phe-246 (Glu). The differences in side-chain structure, charge, and hydrophobicity are major and readily explain why $\alpha_X\beta_2$ and $\alpha_M\beta_2$ bind to different regions of iC3b.

Our studies on $\alpha_X\beta_2$ here extended a previous EM study on the $\alpha_X\beta_2$ ectodomain (19) by using the isolated αI domain and by identifying the location of a secondary binding site in iC3b. The isolated αI domain bound near the interface of the MG3 and MG4 domains in iC3b and C3c and less frequently to an additional, secondary site near the C345C knob in C3c. We were able to confirm binding to the secondary site by using the intact $\alpha_X\beta_2$ ectodomain in both iC3b and C3c. Although we did not observe the secondary site using the αI domain with iC3b, the technical limitations of multivariate K-means classification may have been responsible for a failure to resolve both variation among particles in position of the TED and variation in whether a second αI domain was bound in class averages. The TED is larger than the αI domain and, thus, more dominant in K-means classification. We previously experienced similar dominance of the $\alpha_X\beta_2$ ectodomain over the TED: In $\alpha_X\beta_2$ complexes with iC3b, the TED was not resolved, whereas averaging iC3b particles in the same fields that were not bound to $\alpha_X\beta_2$ resolved the TED (19).

The secondary binding site near the C345C knob resolved here both with binding of the α_X αI domain to C3c and binding of the $\alpha_X\beta_2$ ectodomain to iC3b and C3c is adjacent to the CUB domain linkage to the MG key ring. This region becomes exposed when the CUB domain is cleaved in conversion of C3b to iC3b. Thus, the secondary binding site may be relevant in physiologic recognition of iC3b. Because $\alpha_X\beta_2$ recognizes negatively charged residues in proteolyzed or denatured proteins as a danger receptor (26), it is reasonable to ask whether negatively charged regions are near the secondary recognition site. One candidate is the cleaved terminus of the CUB domain that precedes the MG8 domain, which is present in both iC3b and C3c. The terminal sequence is SEETKENEG and, thus, rich in acidic glutamic residues. Furthermore, this segment is disordered in the C3c crystal structure (31), consistent with recognition by $\alpha_X\beta_2$ of denatured proteins and the appearance of the α_X αI domain on either side of the C345C knob in class averages. We found that two $\alpha_X\beta_2$ ectodomain molecules could simultaneously bind to the primary site near MG3 and MG4 and the secondary site near the C345C knob on a single iC3b molecule. The use of both sites may contribute to more avid recognition by $\alpha_X\beta_2$ (CR4) of iC3b.

In addition to our main focus here on iC3b recognition, our studies also provide insights into promiscuous recognition and headpiece opening by $\alpha_M\beta_2$. Ligand binding through the αI domain was associated with swing-out of the β-subunit hybrid domain as visualized by the open headpiece conformation in EM. Studies with Fabs to the β_2 subunit that stabilize the open conformation show that they greatly increase affinity of $\alpha_L\beta_2$ for its ligand ICAM-1 and of $\alpha_X\beta_2$ for iC3b (32, 33). Here, the principle that headpiece opening is associated with the high-affinity state of the αI domain (Fig. 1*B*) has been extended to integrin $\alpha_M\beta_2$, and was demonstrated for both binding of $\alpha_M\beta_2$ to a specific ligand (iC3b) and a promiscuous ligand ($\alpha_M\beta_2$).

Specific and promiscuous recognition by $\alpha_M\beta_2$ are brought into focus here by its ability to both bind iC3b and self-associate into dimers. Integrin $\alpha_M\beta_2$ has been found to bind a range of ∼40 different proteins, glycans including heparin, and denatured proteins (reviewed in ref. 25). Nonetheless, $\alpha_M\beta_2$ (CR3) is highly selective for iC3b. $\alpha_M\beta_2$ on the surface of myelomonocytic cells selectively rosettes with cells sensitized with iC3b but not with cells bearing IgM, C3b, or C3d (4, 5). The latter is equivalent to the TED.

Our studies on $\alpha_M\beta_2$ show that it not only binds through its αI domain to the TED in iC3b, but also binds through its head region to the C345C-proximal region of the C3c moiety. The recent crystal structure of the α_M αI domain bound to TED was validated with measurement of a micromolar K_D value and elimination of binding with mutation of a key recognition residue in TED (21). However, because binding to TED (C3d) did not match the specificity of $\alpha_M\beta_2$ for iC3b, this study raised two possibilities: (*i*) Binding to TED might reflect the promiscuity of $\alpha_M\beta_2$ and not be related to iC3b recognition. (*ii*) As suggested by the authors, binding of the αI domain to TED might represent only one of two interactions, with the second interaction providing selectivity for iC3b over C3d. Although previous structural work on recognition by $\alpha_M\beta_2$ of iC3b was with the isolated α_M αI domain, our current work is with the $\alpha_M\beta_2$ headpiece and provides evidence for such a second interaction.

In $\alpha_M\beta_2$ complexes with iC3b, despite the flexible linkage connecting the αI domain-bound TED to the C3c moiety through the unfolded, partially cleaved CUB domain, almost all class averages showed a similar orientation of the C3c moiety, with the thick side of the MG key ring facing the integrin and the C345C knob-proximal region of the C3c moiety touching or near to the β-propeller/βI domain portion of the $\alpha_M\beta_2$ head. An interaction in this region of iC3b with the β-propeller/βI domain region of $\alpha_M\beta_2$ is strongly suggested by the preponderance of class averages with this orientation and the contrast with the random orientation of the TED relative to C3c moiety in class averages of iC3b alone. Evidence for a specific interaction in this region is further strengthened by the uniform orientation of the $\alpha_M\beta_2$ headpiece with its β-subunit side proximal to the C3c moiety of iC3b. Because in iC3b the TED is flexibly tethered through the unfolded remnant of the CUB domain to the C3c moiety, TED flexibility should generate random orientations of the C3c moiety relative to the $\alpha_M\beta_2$ headpiece if there were no interactions other than those between the αI domain and TED. In summary, both the similar positions of the C3c moiety relative to the $\alpha_M\beta_2$ headpiece in all well-resolved class averages of the iC3b–$\alpha_M\beta_2$ headpiece complex, and the orientation with the thick side of the MG domain ring in C3c facing the headpiece and the β-subunit side of the headpiece facing the C3c moiety, support an additional stabilizing interaction between the C345C-proximal region of the C3c moiety and the β-propeller/βI domain portion of the $\alpha_M\beta_2$ head.

An interaction of the knob-proximal region of the MG domain ring of iC3b with the β-propeller/βI domain region of $\alpha_M\beta_2$ is consistent with previous evidence that these regions contribute to CR3 function. When the αI domain is deleted from $\alpha_M\beta_2$, it retains partial ability to bind iC3b but not several other ligands, and residual CR3 function is completely inhibited by an antibody to the β-propeller domain (22). The antibody binds an epitope that includes a βI domain-proximal loop in blade (β-sheet) 6 of the β-propeller domain (34, 35). Mutagenesis has suggested a role for nearby blade 4 of the β-propeller domain and the βI domain in iC3b recognition (23, 24). Moreover, the recognition site near the C345C knob on the MG key ring of the C3c moiety is consistent with previous mutational data on CR3 recognition of iC3b. Mutation of iC3b residues 736 and 737, which localize to the α′NT segment, markedly diminishes recognition of iC3b by $\alpha_M\beta_2$ (36). Notably, α′NT localizes to the thick side of the C3c key ring adjacent to the C345C knob (Fig. 1*A*), i.e., the same region of iC3b that we find interacts with the β-propeller/βI domain region of $\alpha_M\beta_2$. Taken together, the mutational and antibody inhibition data on integrin $\alpha_M\beta_2$, the mutational data on iC3b, and our EM data on $\alpha_M\beta_2$ complexes with iC3b support a model in which the specificity of $\alpha_M\beta_2$ for iC3b derives from bipartite binding of the αI domain and β-propeller/βI domain of $\alpha_M\beta_2$ to the TED and C3c moieties, respectively, of iC3b.

Interestingly, we were also able to compare here the selective interaction of $\alpha_M\beta_2$ with iC3b to a promiscuous self-association with $\alpha_M\beta_2$. Notably, $\alpha_M\beta_2$ self-associates in a reciprocal, symmetric interaction. Thus, the particular promiscuous interaction visualized here was favored by the greater avidity of a dimeric than a monomeric interaction. Despite the difference in avidity, when $\alpha_M\beta_2$ and iC3b were mixed together, recognition of iC3b predominated over self-association, consistent with the selectivity of $\alpha_M\beta_2$ for iC3b compared with other C3 fragments.

In summary, the direct comparisons here between $\alpha_X\beta_2$ (CR4) and $\alpha_M\beta_2$ (CR3) show that although these integrins are close relatives of one another, they bind to different sites on iC3b and, therefore, appear to have independently evolved their specificity for iC3b. There is extensive overlap in expression of these leukocyte integrins on cell types, with both expressed on macrophages and neutrophils, whereas $\alpha_X\beta_2$ is selectively expressed on dendritic cells (10, 11). Remarkably, the primary binding site of $\alpha_X\beta_2$ on the thin side of the C3c key ring lies distal from the $\alpha_M\beta_2$ binding site on the TED domain and thick side of the C3c key ring and comparison of class averages of $\alpha_X\beta_2$ and $\alpha_M\beta_2$ complexes with iC3b (Figs. 2 and 3) suggest that no overlap between the integrins would occur upon simultaneous binding to the same iC3b molecule. The recognition of independent sites by CR3 and CR4 on iC3b provides greater diversity in recognition of opsonized pathogens and immune complexes, and may also allow cooperative interactions between the two integrins.

Materials and Methods

Integrin α_X αI Domain. The α_X αI domain (residues E130 to G319 with F273S and F300A mutations) was expressed in pET28a with a 6 His tag at the N terminus in *Escherichia coli* BL 21(DE3) cells. Expression was induced with 1 mM isopropyl β-D-thiogalactopyranoside for 24 h at 16 °C. Washed bacteria were sonicated in 50 mM Tris pH 8.0, 300 mM NaCl, 10% (vol/vol) glycerol, and 1 mM phenylmethanesulfonyl fluoride. Protein was purified with Ni-NTA resin (Qiagen) and then by gel filtration on a Superdex 200 10/300 column (GE Healthcare) in 20 mM Tris pH 8.0, 300 mM NaCl, 10% (vol/vol) glycerol.

Integrin $\alpha_M\beta_2$ Headpiece. The cDNA encoding the mature residues 1–752 of α_M was cloned into ET11 vector, which was derived from ET1 vector (34). The cDNA encoding the signal sequence and mature residues 1–460 of β_2 subunit was cloned into pEF1-puro vector as described (37). HEK293 cells were cotransfected with expression constructs, and protein was expressed and purified as described (38).

Preparation of Complement iC3b and C3c. Human C3 was purified as described (39). iC3b was prepared according to the literature (40) with slight modification. Generally, the C3 was digested by trypsin to generate C3b and then treated with Factor H/I to generate iC3b. Outdated human plasma (500 mL, stored for several weeks at 4 °C) was treated with 25 mg of zymosan (Complement Technology) for 5 d at 37 °C. C3c was purified by polyethylene glycol precipitation, anion exchange chromatography (DEAE Sephacel, GE Healthcare), cation exchange chromatography (SP fast flow Sepharose, GE Healthcare) and size-exclusion chromatography (Superdex 200 16/60, GE Healthcare) as described (31). C3c was finally stored in buffer containing 20 mM Tris pH 7.4, 150 mM NaCl, 2 mM $MgCl_2$.

Negative-Stain EM. Purified α_X αI domain was mixed with iC3b or C3c at a molar ratio of 10:1 with $MgCl_2$ brought to a final concentration of 2 mM. Complexes were purified by using a Superdex 200 10/300 column (GE Healthcare) in 20 mM Hepes pH 7.4, 150 mM NaCl, and 2 mM $MgCl_2$. The $\alpha_M\beta_2$ headpiece was mixed with iC3b or C3c at a molar ratio of 1:4 in presence of 1 mM $MnCl_2$ and 0.2 mM $CaCl_2$. Complexes were purified with Superdex 200 chromatography, 20 mM Hepes pH 7.4, 150 mM NaCl, 1 mM $MnCl_2$, and 0.2 mM $CaCl_2$. Peak fractions were adsorbed to glow-discharged carbon-coated copper grids, washed with deionized water, and stained with freshly prepared 0.75% uranyl formate. Low-dose images were acquired with an FEI Tecnai-12 transmission electron microscope at 120 kV and a nominal magnification of 67,000× or a Tecnai G^2 Spirit BioTWIN transmission electron microscope at 80 kV and a nominal magnification of 68,000×. Image processing was performed with SPIDER and EMAN as described (19). Five thousand to seven thousand particles were picked interactively and subjected to multireference alignment and K-means classification specifying 50 classes. Cross-correlation was as described (19). The projection of open $\alpha_M\beta_2$ headpiece was generated by using a modeled open form $\alpha_x\beta_2$ headpiece, which contains α_x from ref. 30 and open β from ref. 41.

ACKNOWLEDGMENTS. This work was supported by NIH Grants HL103526 (to J.-H.W.) and AI72765 (to T.A.S.).

1. Walport MJ (2001) Complement. First of two parts. *N Engl J Med* 344(14):1058–1066.
2. Berger M, Gaither IA, Frank MM (1981-1982) Complement receptors. *Clin Immunol Rev* 1(4):471–545.
3. Law SK, Dodds AW (1997) The internal thioester and the covalent binding properties of the complement proteins C3 and C4. *Protein Sci* 6(2):263–274.
4. Beller DI, Springer TA, Schreiber RD (1982) Anti-Mac-1 selectively inhibits the mouse and human type three complement receptor. *J Exp Med* 156(4):1000–1009.
5. Ross GD, et al. (1983) Generation of three different fragments of bound C3 with purified factor I or serum. II. Location of binding sites in the C3 fragments for factors B and H, complement receptors, and bovine conglutinin. *J Exp Med* 158(2):334–352.
6. Bilsland CAG, Diamond MS, Springer TA (1994) The leukocyte integrin p150,95 (CD11c/CD18) as a receptor for iC3b. Activation by a heterologous β subunit and localization of a ligand recognition site to the I domain. *J Immunol* 152(9):4582–4589.
7. Micklem KJ, Sim RB (1985) Isolation of complement-fragment-iC3b-binding proteins by affinity chromatography. The identification of p150,95 as an iC3b-binding protein. *Biochem J* 231(1):233–236.
8. Lin Z, et al. (2015) Complement C3dg-mediated erythrophagocytosis: Implications for paroxysmal nocturnal hemoglobinuria. *Blood* 126(7):891–894.
9. Inada S, et al. (1983) C3d receptors are expressed on human monocytes after in vitro cultivation. *Proc Natl Acad Sci USA* 80(8):2351–2355.
10. Luk J, Luther E, Diamond MS, Springer TA (1995) Subunit specificity and epitope mapping of Mac-1 and p150,95 mAb using chimeric CD11b x CD11c transfectants. *Leucocyte Typing V: White Cell Differentiation Antigens*, eds Schlossman SF, et al. (Oxford Univ Press, New York), pp 1599–1601.
11. Luk J, Springer TA (1995) CD11b cluster report. *Leucocyte Typing V: White Cell Differentiation Antigens*, eds Schlossman SF, et al. (Oxford Univ Press, New York), pp 1588–1590.
12. Gahmberg CG, Tolvanen M, Kotovuori P (1997) Leukocyte adhesion–structure and function of human leukocyte beta2-integrins and their cellular ligands. *Eur J Biochem* 245(2):215–232.
13. Dupuy AG, Caron E (2008) Integrin-dependent phagocytosis: Spreading from microadhesion to new concepts. *J Cell Sci* 121(11):1773–1783.
14. Anderson DC, Springer TA (1987) Leukocyte adhesion deficiency: An inherited defect in the Mac-1, LFA-1, and p150,95 glycoproteins. *Annu Rev Med* 38:175–194.
15. Tang T, et al. (1997) A role for Mac-1 (CDIIb/CD18) in immune complex-stimulated neutrophil function in vivo: Mac-1 deficiency abrogates sustained Fcgamma receptor-dependent neutrophil adhesion and complement-dependent proteinuria in acute glomerulonephritis. *J Exp Med* 186(11):1853–1863.
16. Springer TA, Dustin ML (2012) Integrin inside-out signaling and the immunological synapse. *Curr Opin Cell Biol* 24(1):107–115.
17. Diamond MS, Garcia-Aguilar J, Bickford JK, Corbi AL, Springer TA (1993) The I domain is a major recognition site on the leukocyte integrin Mac-1 (CD11b/CD18) for four distinct adhesion ligands. *J Cell Biol* 120(4):1031–1043.
18. Michishita M, Videm V, Arnaout MA (1993) A novel divalent cation-binding site in the A domain of the beta 2 integrin CR3 (CD11b/CD18) is essential for ligand binding. *Cell* 72(6):857–867.
19. Chen X, Yu Y, Mi LZ, Walz T, Springer TA (2012) Molecular basis for complement recognition by integrin $\alpha_X\beta_2$. *Proc Natl Acad Sci USA* 109(12):4586–4591.
20. Vorup-Jensen T (2012) Surface plasmon resonance biosensing in studies of the binding between β_2 integrin I domains and their ligands. *Methods Mol Biol* 757: 55–71.
21. Bajic G, Yatime L, Sim RB, Vorup-Jensen T, Andersen GR (2013) Structural insight on the recognition of surface-bound opsonins by the integrin I domain of complement receptor 3. *Proc Natl Acad Sci USA* 110(41):16426–16431.
22. Yalamanchili P, Lu C, Oxvig C, Springer TA (2000) Folding and function of I domain-deleted Mac-1 and lymphocyte function-associated antigen-1. *J Biol Chem* 275(29): 21877–21882.
23. Xiong YM, Haas TA, Zhang L (2002) Identification of functional segments within the β2I-domain of integrin αMβ2. *J Biol Chem* 277(48):46639–46644.
24. Li Y, Zhang L (2003) The fourth blade within the β-propeller is involved specifically in C3bi recognition by integrin α M β 2. *J Biol Chem* 278(36):34395–34402.
25. Podolnikova NP, Podolnikov AV, Haas TA, Lishko VK, Ugarova TP (2015) Ligand recognition specificity of leukocyte integrin αMβ2 (Mac-1, CD11b/CD18) and its functional consequences. *Biochemistry* 54(6):1408–1420.
26. Vorup-Jensen T, et al. (2005) Exposure of acidic residues as a danger signal for recognition of fibrinogen and other macromolecules by integrin αXβ2. *Proc Natl Acad Sci USA* 102(5):1614–1619.
27. Lee J-O, Rieu P, Arnaout MA, Liddington R (1995) Crystal structure of the A domain from the α subunit of integrin CR3 (CD11b/CD18). *Cell* 80(4):631–638.
28. Jin M, et al. (2006) Directed evolution to probe protein allostery and integrin I domains of 200,000-fold higher affinity. *Proc Natl Acad Sci USA* 103(15):5758–5763.
29. Nishida N, Walz T, Springer TA (2006) Structural transitions of complement component C3 and its activation products. *Proc Natl Acad Sci USA* 103(52):19737–19742.
30. Sen M, Yuki K, Springer TA (2013) An internal ligand-bound, metastable state of a leukocyte integrin, $\alpha_X\beta_2$. *J Cell Biol* 203(4):629–642.
31. Janssen BJ, et al. (2005) Structures of complement component C3 provide insights into the function and evolution of immunity. *Nature* 437(7058):505–511.
32. Schürpf T, Springer TA (2011) Regulation of integrin affinity on cell surfaces. *EMBO J* 30(23):4712–4727.
33. Chen X, et al. (2010) Requirement of open headpiece conformation for activation of leukocyte integrin αXβ2. *Proc Natl Acad Sci USA* 107(33):14727–14732.
34. Sen M, Springer TA (2016) Leukocyte integrin αLβ2 headpiece structures: The αI domain, the pocket for the internal ligand, and concerted movements of its loops. *Proc Natl Acad Sci USA* 113(11):2940–2945.
35. Lu C, Oxvig C, Springer TA (1998) The structure of the β-propeller domain and C-terminal region of the integrin αM subunit. Dependence on β subunit association and prediction of domains. *J Biol Chem* 273(24):15138–15147.
36. Taniguchi-Sidle A, Isenman DE (1994) Interactions of human complement component C3 with factor B and with complement receptors type 1 (CR1, CD35) and type 3 (CR3, CD11b/CD18) involve an acidic sequence at the N-terminus of C3 alpha′-chain. *J Immunol* 153(11):5285–5302.
37. Nishida N, et al. (2006) Activation of leukocyte β2 integrins by conversion from bent to extended conformations. *Immunity* 25(4):583–594.
38. Dong X, Hudson NE, Lu C, Springer TA (2014) Structural determinants of integrin β-subunit specificity for latent TGF-β. *Nat Struct Mol Biol* 21(12):1091–1096.
39. Sottrup-Jensen L, Andersen GR (2014) Purification of human complement protein C5. *Methods Mol Biol* 1100:93–102.
40. Alcorlo M, et al. (2011) Unique structure of iC3b resolved at a resolution of 24 Å by 3D-electron microscopy. *Proc Natl Acad Sci USA* 108(32):13236–13240.
41. Xiao T, Takagi J, Coller BS, Wang JH, Springer TA (2004) Structural basis for allostery in integrins and binding to fibrinogen-mimetic therapeutics. *Nature* 432(7013):59–67.